

A Computational Model of Acute Focal Cortical Lesions

Sharon Goodall, MS*, James A. Reggia, MD PhD*, Yinong Chen, MS*,
Eytan Ruppin, MD PhD[†] and Carol Whitney, MS*

Depts. of Neurology and Computer Science, Inst. Adv. Comp. Studies
University of Maryland*

Depts. of Computer Science and Physiology
Tel Aviv University[†]

Correspondence:

Dr. James A. Reggia
Dept. of Neurology
University of Maryland Hospital
22 S. Greene St
Baltimore MD 21201

Phone: (301) 405-2686

Fax: (301) 405-6707

E-mail: reggia@cs.umd.edu

MS#4216-D-1996, August 8, 1996; Revision #1

Approximate word count: 6550

Acknowledgement: This work was supported by NINCDS awards NS 29414 and NS 16332. The authors thank Michael Sloan and Steve Kittner, and the anonymous reviewers, for helpful comments on this work.

A Computational Model of Acute Focal Cortical Lesions

Heading Computational Model of Cortical Lesions

Abstract

Background and Purpose: Determining how cerebral cortex adapts to sudden, focal damage is important for gaining a better understanding of stroke. In this study we used a computational model to examine the hypothesis that cortical map reorganization following a simulated infarct is critically dependent upon perilesion excitability, and to identify factors that influence the extent of post-stroke reorganization.

Methods: A previously reported artificial neural network model of primary sensorimotor cortex, controlling a simulated arm, was subjected to acute focal damage. The perilesion excitability and cortical map reorganization were measured over time and compared.

Results: Simulated lesions to cortical regions with increased perilesion excitability were associated with a remapping of the lesioned area into the immediate perilesion cortex, where responsiveness increased with time. In contrast, when lesions caused a perilesion zone of decreased activity to appear, it enlarged and intensified with time, with loss of the perilesion map. Increasing the assumed extent of intracortical connections produced a wider perilesion zone of inactivity. These effects were independent of lesion size.

Conclusions: These simulation results suggest that functional cortical reorganization following an ischemic stroke is a two phase process in which perilesion excitability plays a critical role.

Keywords: Computer Models; Cerebral Infarction; Stroke, ischemic

As computational methods for brain modeling have advanced during the last several years there has been an increasing interest in adopting them to study disorders in neurology, neuropsychology, and psychiatry. For example, models of Alzheimer’s disease, epilepsy, aphasia, dyslexia, and schizophrenia have been studied recently to obtain a better understanding of the underlying pathophysiological processes [1].

The complexity of events in stroke suggests that computational models can be powerful tools for its investigation, much as they are in the analysis of other complex systems (global climate prediction, geological exploration, etc.). Ultimately, one seeks a sufficiently powerful model that can be used to understand better the acute post-stroke changes in the ischemic penumbra, to determine which factors lead to worsening or recovery from stroke, and to suggest new pharmacologic interventions and rehabilitative actions that could improve stroke outcome. However, the complexity of stroke pathophysiology, and the limitations of current modeling technology and neuroscientific knowledge, make it impractical to create immediately a detailed, large scale model of the brain and all of the effects of a major stroke. Here we consider the more limited yet still challenging objective of creating a computer model of circumscribed regions of cerebral cortex and of small, ischemic lesions. We further consider only neuronal activation effects of acute lesions on cortical maps due to disruption of neural elements.

Many past computational models of the cerebral cortex have concentrated on map formation since this is a prevalent organizational aspect of the mammalian brain. Cortical maps represent similar inputs close to one another in the cortex, and can be divided into topographic maps and feature maps [2, 3]. For *topographic maps*, similarity of input patterns is measured in terms of their geometric proximity. For *feature* or *computational maps*, the similarity measure can represent any functional correspondence of the input patterns. For example, in visual cortex a feature map of stimulus orientation varies systematically over the cortical surface, embedded in a topographic (retinotopic) map.

While both topographic maps and feature maps have been modeled computationally in the past [1], previous studies involving acute focal cortical lesions have focused on topographic somatosensory maps [4, 5, 6]. Conceptually, these latter models simulate the projection of the hand’s tactile sensory neurons onto a two-dimensional region of primary somatosensory cortex. Neural activity and synaptic changes are modeled mathematically. Initially, thalamocortical synaptic strengths are random, so a precise cortical map of the

hand surface does not exist. The models undergo a developmental *training period* during which synaptic modifications occur as random stimuli are applied to the hand. Synaptic strengths change over time according to a competitive Hebbian rule: correlated presynaptic and postsynaptic activity lead to strengthening of a synapse, while uncorrelated activity leads to weakening. As a result, the receptive fields of cortical elements in model cortex change with time, and a topographic cortical map appears in which adjacent cortical elements are activated by adjacent stimuli on the hand surface.

After a model is trained as described above, a focal lesion is introduced into the developed topographic map in primary somatosensory cortex. This causes the map to reorganize such that the sensory surface originally represented by the lesioned area spontaneously reappears in adjacent cortical areas, as has been seen experimentally in animal studies [7]. Two key hypotheses emerged from this modeling work. First, post-lesion map reorganization is a two-phase process, consisting of a rapid phase due to the dynamics of neural activity and a longer-term phase due to synaptic plasticity. Second, increased perilesion excitability is necessary for useful map reorganization to occur.

These previous simulation studies, as well as others [8], indicate the important role of intracortical interactions in post-lesion brain reorganization. Specifically, following a *structural lesion* that simulates a region of damage and neuronal death, a secondary *functional lesion* can arise in adjacent cortex due to loss of synaptic connections from the damaged area to surrounding intact cortex. In the following we use the term “functional lesion” in this limited sense and not to indicate the ischemic penumbra.

In the work reported in this paper, we examined these two map reorganization hypotheses through simulations with a new cortical model. We used a recently developed computational model of primary sensorimotor cortex that controls the positioning of a simulated arm in three-dimensional space [9]. This model is substantially more complex than the somatosensory cortex model describe above, but neural activation dynamics and synaptic modifications are governed by similar principles and mathematical equations. Starting with initially random synaptic strengths, the model is trained by letting synaptic changes occur while random stimuli are applied to the motor cortex. As a result, maps form in the two cortical regions represented in the model: proprioceptive sensory cortex and primary motor cortex (MI). Unlike the previous computational models of somatosensory cortex described above that were subjected to simulated focal lesions [4, 5, 6], the maps involved here are

feature maps and involve motor output as well as sensory input information. In simulations with the model, we examined and compared both perilesion excitability and cortical map reorganization, immediately after a lesion and over the long term. The results obtained support the two hypotheses given above. In the following, we describe these results, correlate our hypotheses with the findings, and describe how they may influence the fate of the ischemic penumbra in stroke.

METHODS

Model Description

The computational model used in this study is a recently reported artificial neural network model of primary sensorimotor cortex [9]. It consists of two parts: a simulated arm that moves in three dimensional space, and a closed-loop of neural elements that controls and senses arm positions. Each neural element in the model represents a population of real neurons, not a single neuron. The structure of the model is illustrated in Fig. 1.

Fig. 1 About Here

The transformation of activity in lower motor neurons to proprioceptive sensory neural activity is generated using a simulated arm (bottom of Fig.1). This model arm is a significant simplification of biological reality [9, 10]. It consists of upper and lower arm segments, connected at the elbow. It has six generic muscle groups, each of which corresponds to multiple muscles in a real arm. Abductor and adductor muscles move the upper arm up and down through 180° , respectively, while flexor and extensor muscles move it forward and backward through 180° , respectively. The lower arm flexes and extends as much as 180° , controlled by lower arm flexor and extensor muscles. Activation of the lower motor neuron elements place the model arm into a specific spatial position. The simulated arm then generates input signals to the cortex via the proprioceptive neuron elements that indicate the length and tension of each individual muscle group (see Fig. 1).

Activation flows in a closed loop through four sets of neural elements: primary motor cortex (MI), lower motor neurons, proprioceptive neurons, proprioceptive cortex (PI), and back to MI (Fig. 1). Activity in lower motor neurons sets the arm position, which in turn determines the length and tension of six simulated muscle groups. We use the non-standard

abbreviation PI to designate the region of primary somatosensory cortex receiving proprioceptive input from the upper extremity; this roughly corresponds to Brodmann area 3a [11]. The twelve receptor elements in the proprioceptive input layer are fully connected to PI; they provide six muscle length and six muscle tension measures. A length element becomes active when the corresponding muscle is stretched, while a tension element activates when the corresponding muscle produces tension through active contraction. Biologically, length (stretch) is measured by the receptors in muscle spindles, while muscle tension is measured by receptors in Golgi tendon organs [12].

The PI and MI layers are both two dimensional arrays of elements with lateral (horizontal) intracortical connections. Each element of these layers represents a cortical column, and is connected to its immediate neighboring elements in a hexagonal tessellation. To avoid edge effects, elements on the edges of the cortical sheet are connected with their corresponding neighbor elements on the opposite edges, forming a torus, as is often done in models of this sort. Each element of PI sends synaptic connections to its corresponding element in MI and to surrounding elements in MI within a radius 4, providing a coarse topographic ordering for the connections from PI to MI. This pattern of connectivity is motivated by previous experimental studies that have demonstrated topographic ordering of excitatory connections from primary sensory cortex to MI [13, 14]. Each MI element is fully connected to the lower motor neurons.

Each neural element i in the model has an associated activation level $a_i(t)$, representing the mean firing rate of neurons in that element at time t (see Appendix). A “Mexican Hat” pattern of cortical activity, i.e., a central region of excitation with a surrounding annular region of inhibition as occurs experimentally [15, 16], appears in response to a localized excitatory cortical input. This response is produced by a competitive model of cortical dynamics that has been previously used on multiple occasions for this purpose [4, 10, 17].

Initially, weights on all interlayer connections are randomly assigned, so the initial cortical maps are poorly organized. During simulations, connection weights representing synaptic strengths are modified using an unsupervised learning rule similar to that used in several previous models of cerebral cortex [1, 4, 5, 10]. Only inter-layer connections are changed. The learning rule is both correlational (Hebbian) and competitive: the strengths of synapses between simultaneously active neural elements tend to increase (correlational), while those between elements with uncorrelated activities tend to decrease (competitive).

Synaptic modifications done in this fashion lead to cortical elements with incoming weights (synaptic strengths) whose spatial distribution resembles the input patterns that activate those elements. Since lateral excitatory intracortical connections tend to make nearby cortical elements active simultaneously, neighboring cortical elements develop similar receptive fields and thus a map appears over time.

Map Formation In the Intact Model

The neural model is initialized with small, random weights so that well-formed feature maps are not present in the cortical regions initially. The model is then trained as follows. A patch of external input is repeatedly provided at randomly selected positions in MI (radius 1, intensity 0.3, duration 720 iterations). Two thousand random stimuli to MI, covering the cortical space, are applied to the network during training, after which further training does not produce qualitative changes in the trained weights or the cortical feature maps that appear.

To examine the resultant *proprioceptive maps* in the cortical layers, the two cortical areas are analyzed to determine to which muscle length and tension input each cortical element responds most strongly. Twelve input test patterns are presented, each having only one muscle length or tension element of the proprioceptive input layer activated. Since the proprioceptive input layer elements represent the length and tension of the six muscle groups of the model arm, each test pattern corresponds to the unphysiological situation of having the length or tension of only one muscle group activated (this situation was *never* present with the training patterns). A cortical element is taken to be “maximally tuned” to an arm input element if the activation corresponding to that input element is largest and above a threshold of 0.4 (the distribution of cortical activations was bimodal, with values mostly between 0.0 - 0.25 or 0.6 - 1.0, so our results are relatively insensitive to exact choice of threshold). The pre-lesion feature maps are described in detail in [10, 9] and are summarized briefly here.

Figure 2 about here

Fig. 2 shows which PI and MI cortical elements are maximally responsive to stretch of specific muscles after training. For example, the element in the upper left corner of Fig. 2a is maximally responsive to stretch of the upper arm adductor (D). The input map

in Fig. 2a is for all six muscle groups for the PI cortical layer; the map in Fig. 2c below it is the corresponding input map for MI. Prior to training, elements maximally responsive to the same muscle group’s stretch or tension were irregularly scattered across the map.

Although difficult to see in Fig. 2a and 2c, the maps form clusters of adjacent elements that respond to the same input. This can be better seen in the maps of Fig. 2b and 2d, which show just those elements in Fig. 2a and 2c that are maximally activated by the stretch of the upper arm extensor (E) and upper arm flexor (F), in PI and MI respectively. Fig. 2b illustrates the regular size and spacing of the clusters across the PI layer, and that clusters responsive to antagonist muscles tend to be separated (“E”s and “F”s tend to be pushed apart). PI and MI maps of responsiveness to muscle tension inputs also exhibit uniformity in size and spacing of clusters responsive to the same muscle group. Note that the PI and MI maps of muscle length sensitivity in Fig. 2b and 2d are not aligned, in spite of the fact that there is a rough topographic ordering in connections between PI and MI. The transformation of the map in MI relative to PI arises because multiple clusters of PI elements are active simultaneously. The divergent connections from such nearby active clusters in PI produce a pattern of activity in MI that is not a copy of that in PI, and the synaptic modification rule captures the correlations between these different activity patterns, leading to non-aligned maps [9]. Different maps in the *same* region of cortex can also have interesting relationships. For example, when the length map for PI is compared with the tension map for that layer, it is found that the length map of a particular muscle matches well with the tension map of its antagonist muscle [9]. The maps capture correlated features of input patterns, reflecting the mechanical constraints imposed by the model arm.

In addition to the sensory or input maps in MI, there is simultaneously an MI *motor output map*. The output map is determined by examining each MI element to see which muscle group(s) it activates most strongly. With training, clusters of elements activating the same muscle group appear in this map as well, resembling the distributed nature of motor output maps observed experimentally in animal studies [18]. Further study reveals that the MI input map of a particular muscle’s length matches the MI output map of its antagonist muscle, while the MI input map of a particular muscle’s tension matches the MI output map of its corresponding muscle [9]. The motor output map in MI (not pictured here) thus resembles the proprioceptive input map in Figure 2d very closely, except the E’s and F’s are reversed.

Lesioning the Model

To examine the effects of sudden, focal lesions of varying sizes to the cortex (“simulated ischemic strokes”), two sets of simulations were done in which an area of focal damage was suddenly imposed upon a previously trained network. The first set involved lesions in PI, the second lesions in MI. In both cases, a focal lesion was simulated by clamping the activation levels of a contiguous set of “lesioned” cortical elements permanently at zero. In addition, connections to and from lesioned cortical elements were severed.

The effect of each lesion on the existing proprioceptive and motor maps in the trained, intact cortex was examined twice: immediately after the lesion, and after continually training the network with 2000 additional random input stimuli in MI. Random stimuli were used as we are modeling the natural evolution of post-lesion changes rather than a specific rehabilitative intervention. An analysis of changes in the position of the model arm following cortical stimuli was also made both immediately post-lesion and after further training. All lesion effects were compared with the pre-lesion network as well as with a control network. The control network was an exact copy of the intact pre-lesion network made immediately before lesioning. Training was continued with this unlesioned control model, with additional random input stimuli, so that any map alterations due to continued training alone could be compared to those due to lesioning plus continued training.

To guard against an interaction between lesion effects and the initial state of the model, simulations were done with several different sets of initial random weights. No significant qualitative difference was identified in the lesion results with any initial set of random weights.

RESULTS

Unlesioned Control Model

In the lesioning experiments described below, we always started with a prelesion model that had been trained so that quasi-stable, well-formed maps were present in both sensory and motor cortical regions. We then induced focal structural damage in these models and allowed inter-layer synaptic modifications to continue for 2000 input stimuli. In each case,

a corresponding unlesioned model, starting from the same initial state of well-formed maps, was run as a control to examine the effects of the same 2000 input stimuli and synaptic modifications in the absence of a lesion. As expected, little qualitative change was seen in the control cortical maps with this further training beyond the small shifts of cluster positions in the maps expected with this motor loop model [9].

Figure 3 about here

As with the cortical maps, the positions assumed by the model arm in response to cortical stimuli did not differ significantly between the trained, prelesion model and the control. Fig. 3a shows the model arm in four of six test positions, for both the intact pre-lesion model and the further trained control model, corresponding to “requests” to contract the upper arm extensor, upper arm flexor, upper arm abductor and upper arm adductor. As seen in Fig. 3a, the four arm positions corresponding to these motor cortex stimuli are in the anticipated directions and are virtually indistinguishable for the trained prelesion model (dotted lines) and the further trained control model (hatched lines). The stability of both cortical maps and arm positioning in response to cortical stimuli in the control model indicate that changes seen in the lesioning simulations described below are caused by the lesions themselves.

Focal Lesions in Proprioceptive Cortex

We examined the effects of structural lesions in PI under a variety of conditions. Changes to the feature maps in PI were observable immediately after a structural lesion occurred in this layer, as the first phase of a two-phase reorganization process. Following the primary structural lesion in PI, the activity of surrounding elements was decreased, forming a secondary functional lesion. For example, Fig. 4a shows a perilesion zone of relatively inactive cortical elements (marked by “-”s) seen immediately following an 8x8 focal lesion; these elements do not respond to the stretch of any of the muscles above a threshold of 0.4.

Figure 4 about here

The second phase of reorganization occurred more slowly with continued synaptic changes during the post-lesion period. With time, as the map reorganized in the context

of continued proprioceptive input and synaptic changes, the functional lesion gradually enlarged. For example, with an 8x8 structural lesion there was a 77% increase in perilesion inactivity at distances 1 and 2 from the lesion edge over the long term (see Fig. 4b, in comparison with Fig. 4a). Similar changes were observed with the proprioceptive map of muscle tension. Over time, clusters of elements responsive to the stretch of a particular muscle also shifted position in the feature map.

The functional lesion effects described above occurred largely independently of structural lesion size in PI. They are representative of the effects observed with lesions that varied incrementally in size from 2x2 to 8x8. The dynamics of these functional lesions can be analyzed further by examining the mean activation level of cortical elements, averaged over all of the test input patterns. There was an essentially uniform pre-lesion mean activation of the PI elements of roughly 0.12. Immediately following the structural lesion, the mean activation level of cortical elements directly adjacent to the lesion site dropped to 0.08, about 70% of its pre-lesion value. With additional synaptic modifications following the lesion, these perilesion effects in the PI layer were intensified (about 25% of prelesion value) and shifted outwards.

Further examination of the model, following lesions in PI, reveals that perilesion cortical elements were activated essentially the same amount for all input stimuli, in contrast with the prelesion cortex where elements were activated selectively for some specific input stimuli but not others. This uniformity occurred as the result of the loss of excitatory support from cortical elements in the structural lesion via intracortical connections. As the map reorganized following the lesion, the weights to these perilesion cortical elements tended to become uniform.

We attempted to prevent the spread of the perilesion functional deficit by providing a small uniform external input to elements at a distance 1 from the lesion during the post-lesion period of continued synaptic modifications. We did this to confirm that it is the low activation levels in the perilesion elements that leads to the spread of the functional deficit. This change arrested the spread of the perilesion functional deficit: there was significantly more reorganization in the map at distance 2 from the lesion. However, when synaptic modifications were subsequently allowed to continue even further without the increased external input, all gains made in arresting the spread of the functional deficit were lost.

Immediately following the larger structural lesions (5x5 and larger) in PI, an irregularly shaped area of inactive motor cortex elements appeared in the center of the sensory maps of the MI layer, and did not resolve with further training. Given the coarsely topographic projections from PI to MI (projections from PI to MI elements within a radius 4), the observed inactive zone in the center of the motor cortex sensory map is expected, and can be viewed as an example of diaschisis. In addition to these effects on the sensory maps of the MI layer, larger PI lesions produced a central region in the motor output map that did not activate any muscle groups in the lower motor neuron layer. This was due to the loss of excitatory input to this region from the corresponding lesioned area in PI. The percentage of MI elements activating one or more muscle group(s) in the motor output maps was 77% prior to lesioning. This decreased with larger PI lesions (5x5 and larger), e.g., with an 8x8 PI lesion, the percentage dropped to 68% over time.

The decrease in motor output map responsiveness with lesions of increasing size led to “weakness” of the model arm following a lesion in PI. Fig. 3b shows the arm position for the same four test inputs to MI as in Fig. 3a, for an 8x8 focal lesion in PI. Immediately post-lesion, a measurable shift was observed in arm positions away from their pre-lesion position and towards the neutral, resting position of the arm. For example, the elbow position immediately post-lesion for the upper arm flexor test was 20° away from its pre-lesion position, revealing a weakened flexor response. Similar weakened responses were seen with the contraction tests of the abductor, adductor and lower arm flexor immediately post-lesion. This occurred due to functional loss of MI elements that activated each muscle group. However, over time with continued cortical plasticity, the arm positions for all test inputs realigned with their pre-lesion positions, representing essentially complete “recovery”. With larger PI lesions, e.g., 16 x 16, such recovery was incomplete.

Focal Lesions in Motor Cortex

A separate set of simulations was performed to study reorganization of the MI cortical maps following focal structural lesions of varying sizes in MI (2x2 to 8x8). For sufficiently large lesions, reorganization after a structural lesion in MI was seen in both the MI sensory and motor output maps. Immediately after such large focal lesions to MI, both the stretch and tension sensory maps for MI adjusted so that there was an increase in the number of responsive elements in normal cortex near the lesion edge. In contrast to PI lesions, no

perilesion zone of decreased activation was present. This reorganization can be seen by comparing the MI sensory map for muscle stretch in Fig. 5a with the corresponding map in Fig. 2c. At distances 1 and 2 from the lesion edge there was an increase in the number of responsive elements over pre-lesion levels, from 91% pre-lesion to 96% immediately after this 8x8 lesion. Although the change in absolute numbers of responsive elements is small, it accurately reflects a substantial increase in mean activation levels of all elements averaged over all inputs in this perilesion zone (from 0.14 before lesion to 0.21 after). Over time, the distance 1 and 2 responsiveness stabilized at 99%, as is seen in Fig. 5b. Overall rates of responsiveness for the MI sensory maps increased slightly immediately following the onset of the lesion, but then dropped back to prelesion levels with continued post-lesion synaptic modifications.

Fig. 5 about here

This post-lesion reorganization result is similar to results of prior studies of structural lesions to cortical layers with topographically-ordered somatosensory inputs [5]. In this context, it is important to note that the topographically-ordered connections between PI and MI in this current model are similar to those between thalamus and sensory cortex in the earlier model (projections from PI to corresponding MI elements are made within a radius 4).

Like the MI sensory maps described above, the MI output map in residual intact cortex experienced an increase in relative activity. The number of MI elements activating one or more muscle group(s) increased following a MI lesion of sufficient size (4x4 and larger). For an 8x8 lesion, the percentage of remaining MI elements activating one or more muscle group(s) increased from 77% to 86% of intact elements. This affected the positioning of the model arm as well, when tested with six external inputs to MI. As seen in Figure 3c, with a 16x16 focal lesion in MI the arm position revealed a weakened response immediately post-lesion. For example, the elbow position immediately post-lesion for the upper arm flexor test was 15° away from its pre-lesion position, roughly in the direction of the resting position. Further post-lesion synaptic modifications in the presence of the MI lesion did not produce a complete realignment of the arm positions with their pre-lesion location, although complete recovery did occur with smaller MI lesions (e.g., 8x8).

The lack of any significant post-lesion reorganization with small MI lesions (2x2 and 3x3) can be attributed to the coarseness of the topographic projections from PI to MI. Each

MI element receives input from 61 PI elements, so with such small MI lesions the distribution of output from PI elements was only minimally perturbed, and perilesion elements continued to experience a distribution of input patterns similar to that before lesioning. As a result their receptive fields, and thus the MI map, remained largely unchanged due to the correlational nature of the synaptic modification rule.

Examination of the feature maps for PI (both post-lesion and with further training) did not reveal any qualitative reorganization following MI lesions, beyond the small shifts of cluster positions expected with this model [9]. While motor output was weakened with larger MI lesions, it did not appear to affect feature map organization in PI.

DISCUSSION

It is currently not well understood how the neural circuits of the cerebral cortex adjust to the sudden structural damage occurring with an ischemic stroke. In this study we induced acute focal lesions in a computational model of primary sensorimotor cortex to examine the resultant functional deficits in surrounding cortex. While such a neural model is a substantial simplification of reality, it is based on generally accepted concepts of cortical structure, activity dynamics and synaptic plasticity. It demonstrates interesting post-lesion effects concerning cortical map reorganization, along with some insight into why these secondary effects arise. Such effects represent testable predictions of the model.

In our simulations, it was observed that focal lesions resulted in a two-phase map reorganization process in the intact perilesion cortical region. The first, very rapid phase was due to changes in activation dynamics, while the second, slow phase was due to synaptic plasticity. Thus, the model makes the prediction that biological perilesion map changes will be demonstrable within a few minutes of a cortical lesion. To our knowledge, while there are a few experimental animal studies that have examined post-lesion cortical map reorganization (see below), none of these have measured maps immediately following the lesion. Recent experimental studies in animals have repeatedly shown map reorganization within minutes following focal deafferentation of cortex [19, 20]; our model predicts that they will occur following cortical lesions as well and provides some details about their nature.

The second prediction of our model is that increased perilesion excitability is neces-

sary for effective map reorganization in cortex surrounding an acute focal lesion. When increased perilesion excitability was present during the first phase of map reorganization, the cortex surrounding the lesion consistently participated in the map reorganization process, even achieving a higher density feature map than in the prelesion cortex. Presumably such effective utilization of surrounding intact cortex following a lesion could contribute to behavioral recovery following an ischemic stroke. On the other hand, when there was decreased excitation in perilesion cortex, this intact cortex consistently did *not* participate in map reorganization, and the perilesion cortex that “dropped out” of the map actually expanded with time due to the normal modifications of synaptic strengths. These very different results, observed here for pure feature maps (PI) and for feature maps involving topographically arranged inputs (to MI from PI), are consistent with similar results obtained in our earlier study involving pure topographic maps [4, 5].

The notion that perilesion excitability is an important factor may prove useful in interpreting animal studies of post-lesion map reorganization. Under some conditions in these studies, functions originally represented in the infarct zone of sensorimotor cortex reappeared or expanded in nearby intact cortex [7, 21, 22], while under other conditions they did not [23]. Our model suggests that assessing perilesion excitability under these differing conditions may shed light on why the different results occur.

The dependence of map reorganization upon perilesion excitability in the model can be explained by examining the synaptic modification rule that produces map formation originally (equation (3) in Appendix). Informally, this rule causes changes to a cortical element’s receptive field 1) at a rate proportional to how active that element is, and 2) such that the receptive field shifts to become more like the pattern of input elements that activate that cortical element. Thus, when the activation of a perilesion element is low, its receptive field changes very slowly and little reorganization occurs. When perilesion activity is high, the receptive field will change quickly and substantial reorganization will occur. In this context, the differences in the input connections to PI and MI account for differences in how these two regions reorganize. In PI, the diffuse afferent inputs have little influence on, and therefore little correlation with, the perilesion elements following a lesion. Thus intact cortical elements adjacent to the original post-lesion functional deficit lose correlated activity from neighbors, become less correlated with specific input patterns, and tend to drop out of the map. In contrast, the coarsely topographic connections from PI

to MI that originally supply the outer region of lesioned cortex have an increased influence on, and become more correlated with, perilesion elements, causing the latter's receptive fields to shift and thus substantial map reorganization to occur.

In the context of these modeling results, it is interesting to note that there does exist direct experimental evidence for increased excitability in intact cortex following a small focal lesion [24]. Such increased excitability has generally been viewed as detrimental, although this is controversial [25]. Our computational model suggests that, in addition, increased excitability may play an important and previously unrecognized role in recovery from stroke. At the very least, the model indicates that further experimental investigation of this issue is warranted and will be useful in obtaining a better understanding of recovery after stroke. In our model, the primary factors determining whether perilesion activity increased or decreased were the extent of divergence of afferents to the cortical region and the ratio of intracortical lateral excitation to inhibition. In other words, in both PI and MI the cortex immediately around the lesion lost excitatory input from the lesioned region. However, the widely divergent inputs to PI were insufficiently powerful to compensate for this loss of perilesion excitation from lateral connections arising in the lesion area, while the much more focused afferents to MI were.

Finally, the results of this study raise more global issues about the role of computational models in stroke research in general. Computational modeling represents a truly novel approach to studying stroke that complements traditional methods and may provide useful guidance for future empirical studies. The results reported here, as well as the related recent modeling results described earlier, provide the first demonstration that nontrivial computational models of ischemic stroke are possible. Of course, these models are substantial simplifications of biological reality. We are currently extending our models to encompass some of the biochemical and metabolic alterations occurring in the ischemic penumbra, with an emphasis on ischemic depolarizations resembling cortical spreading depression. Initial results in modeling cortical spreading depression in *normal* cortex have been encouraging [26]. Ultimately, the utility of such computational models may prove to be their heuristic value in suggesting novel experimental investigations and new approaches to therapeutic and rehabilitative intervention.

References

- [1] J Reggia, E Ruppin, and R Berndt (eds.). *Neural Modeling of Brain and Cognitive Disorders*. World Scientific, 1996.
- [2] E Knudsen, S du Lac, and S Esterly. Computational maps in the brain. *Annual Review of Neuroscience*, 10:41–65, 1987.
- [3] S Udin and J Fawcett. Formation of topographic maps. *Annual Review of Neuroscience*, 11:289–327, 1988.
- [4] G Sutton, J Reggia, S Armentrout, and C D’Autrechy. Map reorganization as a competitive process. *Neural Computation*, 6:1–13, 1994.
- [5] S Armentrout, J Reggia, and M A Weinrich. A neural model of cortical map reorganization following a focal lesion. *Artif. Intel. in Med.*, 6:383–400, 1994.
- [6] J Xing and G Gerstein. Networks with lateral connectivity. *Journal of Neurophysiology*, 75:184–232, 1996.
- [7] W Jenkins and M Merzenich. Reorganization of neocortical representations after brain injury. In F Seil, E Herbert, and B Carlson (eds.), *Progress in Brain Research*, 71, 249, 1987.
- [8] E Ruppin and J Reggia. Patterns of functional damage in neural network models of associative memory. *Neural Computation*, 7:1105–1127, 1995.
- [9] Y Chen and J Reggia. Alignment of coexisting cortical maps in a motor control model. *Neural Computation*, 8:731–755, 1996.
- [10] S Cho and J Reggia. Map formation in proprioceptive cortex. *International Journal of Neural Systems*, 5:87–101, 1994.
- [11] S Wise and J Tanji. Neuronal responses in sensorimotor cortex to ramp displacements. *J. Neurophysiology*, 45:482–500, 1981.
- [12] J Gordon and C Ghez. Muscle receptors and spinal reflexes. In E Kandel, J Schwartz, and T. Jessell (eds.), *Principles of Neural Science*, Elsevier, 564–580, 1991.

- [13] L Porter, T Sakamoto and H Asanuma. Morphological and physiological identification of neurons in the cat motor cortex which receive direct input from the somatic sensory cortex. *Exp. Brain Res.*, 80:209–212, 1990.
- [14] H Yumiya and C Ghez. Specialized subregions in the cat motor cortex. *Exp. Brain Res.*, 53:259–276, 1984.
- [15] R Hess, K Negishi, and O Creutzfeldt. The horizontal spread of intracortical inhibition in the visual cortex. *Experimental Brain Research*, 22:415–419, 1975.
- [16] C Gilbert. Horizontal integration in the neocortex. *Trends in Neurosci.*, 8:160, 1985.
- [17] J Reggia, C D’Autrechy, G Sutton, and M Weinrich. A competitive distribution theory of neocortical dynamics. *Neural Computation*, 4:287–317, 1992.
- [18] J Donoghue, S Leibovic and J Sanes. Organization of the forelimb area in squirrel monkey motor cortex. *Experimental Brain Research*, 89:1–19, 1992.
- [19] J Metzler and P Marks. Functional changes in cat sensory-motor cortex during short-term reversible epidural blocks. *Brain Research*, 177:379–383, 1979.
- [20] C Gilbert and T Wiesel. Receptive field dynamics in adult primary visual cortex. *Nature*, 356:150–152, 1992.
- [21] R Nudo and G Milliken. Reorganization of movement representations in primary motor cortex following focal ischemic infarcts in adult squirrel monkeys. *Journal of Neurophysiology*, 75:2144–2149, 1996.
- [22] M Castro-Alamancos and J Borrel. Functional recovery of forelimb response capacity after forelimb primary motor cortex damage. *Neuroscience*, 68:793-805, 1995.
- [23] R Nudo, B Wise, F SiFuentes and G Milliken. Neural substrates for the effects of rehabilitative training on motor recovery after ischemic infarct. *Science*, 272:1791–1794, 1996.
- [24] R Domann, G Hagermann, M Kraemer, H.-J. Freund and O. Witte, Electrophysiological changes in the surrounding brain tissue of photochemically induced cortical infarcts in the rat. *Neuroscience Letters*, 155:69–72, 1993.

- [25] K Hossmann. Glutamate-mediated injury in focal cerebral ischemia: the excitotoxin hypothesis revised. *Brain Pathology*, 4:23–36, 1994.
- [26] J Reggia and D Montgomery. A computational model of visual hallucinations in migraine. *Computers in Biology and Medicine*, 26:133–141, 1996.

Technical Appendix

We produced a Mexican Hat pattern of lateral interactions using a competitive model of cortical dynamics [5, 10, 17]. The activation level $a_k(t)$ of element k at time t is

$$\frac{da_k(t)}{dt} = c_s a_k(t) + (M - a_k(t))(in_k(t) + ext_k(t)) \quad (1)$$

where $c_s < 0$ is the decay rate, M is the maximum activation, in_k is the activation received by element k from other elements, and ext_k is the external input applied to element k . Omitting t for brevity, the input to element k is

$$in_k = \sum_j c_p \frac{(a_k^p + q)w_{kj}}{\sum_l (a_l^p + q)w_{lj}} a_j. \quad (2)$$

where w_{kj} is the synaptic strength from element j to element k . Constant $c_p > 0$ is the output gain, and parameters p and q influence the degree of peristimulus inhibition. Synaptic weights w_{kj} are altered according to an unsupervised Hebb-like learning rule (competitive learning):

$$\Delta w_{kj} = \eta [a_j - w_{kj}] a_k \quad (3)$$

where η is a small learning constant. Only the weights of the three sets of inter-layer connections are changed; cortico-cortical connections remain constant. Parameter values used here are the same as in [9] with the exception of $c_s = -0.75$ in the MI layer, and a smaller step size $\delta = 0.05$. A detailed description of the training procedure used, the relative insensitivity of results to parameter variations, and the procedures used to assess map formation, are given in [9].

Figure Legends

Figure 1. Structure of the motor control model used in this study.

Figure 2. Maps of the intact proprioceptive (a, b) and motor (c, d) cortex showing which cortical elements respond most strongly to stretch of specific muscles after training. Each cortical element is labeled by a letter indicating the muscle whose stretch (increased length) maximally activates that element: E for upper arm extensor, F for upper arm flexor, B for upper arm abductor, D for upper arm adductor, O for lower arm extensor (“opener”), C for lower arm flexor (“closer”), and “-” for not responsive to stretch of any muscle above an activation threshold of 0.4.

Figure 3 (a) Position assumed by the model arm at rest in the absence of external stimuli (R; thick solid line) and in response to four of six cortical test stimuli. The arm is on the right side of the body and is viewed from the back (S = right shoulder; small circles = hand positions). Each test stimulus provides external input to cortical elements in MI that are most strongly connected to a specific muscle group (here upper arm extensor E, flexor F, abductor B and adductor D). For example, activating upper arm abductor elements in MI elevates the arm to position B. The positions assumed by the arm in response to cortical stimuli are appropriate and indistinguishable for the trained prelesion (dotted lines) and control (cross hatching) states of the model. Similar results are found for the lower arm flexor and extensor (not shown). (b) Arm positions for an 8x8 focal lesion of PI shown pre-lesion (dotted line; largely obscured by overlapping solid lines), immediately post-lesion (dashed line) and after 2000 further random input stimuli in MI (solid line). (c) Arm positions for a 16x16 lesion of MI, pre-lesion (dotted line), immediately post-lesion (dashed line), and after 2000 further random input stimuli in motor cortex layer MI (solid line).

Figure 4. Muscle stretch map of proprioceptive cortex layer PI (above threshold 0.4) for an 8x8 focal lesion of PI (a) immediately post-lesion, and (b) following 2000 further random input stimuli in motor cortex layer MI. Same labeling conventions as in Fig. 2. Asterisks indicate the imposed structural lesion, adjacent “-”s the functional perilesion deficit. A partial but less pronounced “ring” of poorly responsive units is evident at a distance 6 from the lesion (outer border of (b)). This is not an “edge effect”; its genuine presence was verified with a larger cortical region.

Figure 5. Muscle stretch map of motor cortex layer following an 8x8 lesion in MI (a) immediately post-lesion, and (b) after 2000 further input stimuli in MI.

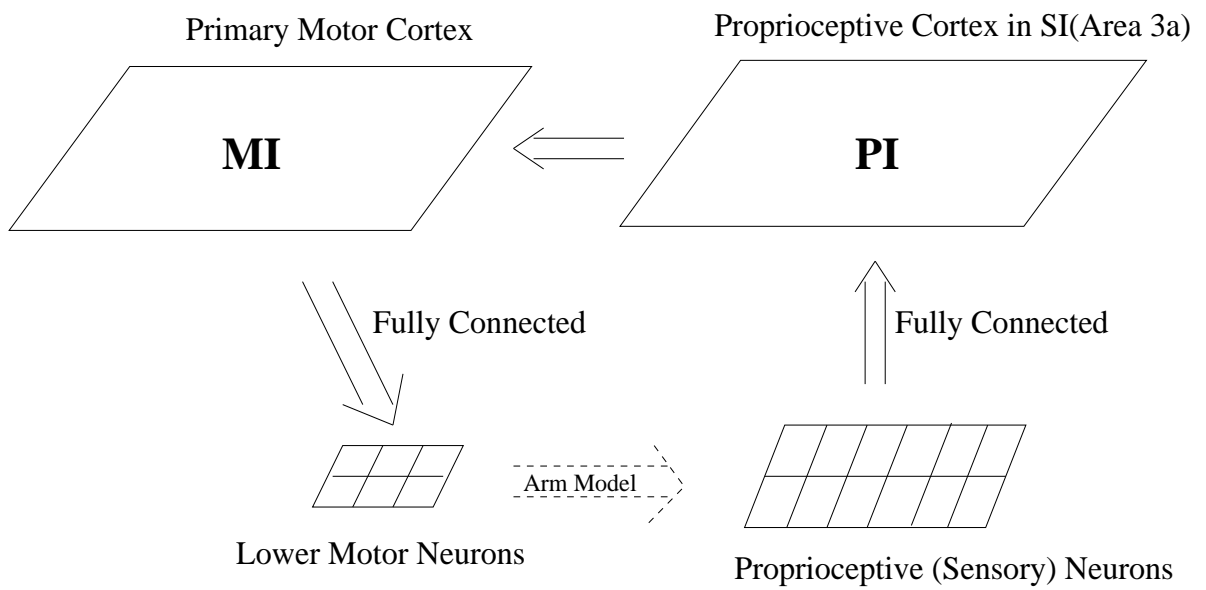


Figure 1:

a.

```

D E O O D D E O O D D E O O D D E O O D
E E O - D E E O - D E E O - D E E O - D
- - F F - - - F F - - - F F - - - F F -
C C F B B C C F B B C C F B B C C F B B
C C - B - C C - B - C C - B - C C - B -
D E O O D D E O O D D E O O D D E O O D
E E O - D E E O - D E E O - D E E O - D
- - F F - - - F F - - - F F - - - F F -
C C F B B C C F B B C C F B B C C F B B
C C - B - C C - B - C C - B - C C - B -
D E O O D D E O O D D E O O D D E O O D
E E O - D E E O - D E E O - D E E O - D
- - F F - - - F F - - - F F - - - F F -
C C F B B C C F B B C C F B B C C F B B
C C - B - C C - B - C C - B - C C - B -
D E O O D D E O O D D E O O D D E O O D
E E O - D E E O - D E E O - D E E O - D
- - F F - - - F F - - - F F - - - F F -
C C F B B C C F B B C C F B B C C F B B
C C - B - C C - B - C C - B - C C - B -

```

b.

```

- E - - - - E - - - - E - - - - E - - -
E E - - - E E - - - E E - - - E E - - -
- - F F - - - F F - - - F F - - - F F -
- - F - - - - F - - - - F - - - - F - -
- - - - - - - - - - - - - - - - - - -
- E - - - - E - - - - E - - - - E - - -
E E - - - E E - - - E E - - - E E - - -
- - F F - - - F F - - - F F - - - F F -
- - F - - - - F - - - - F - - - - F - -
- - - - - - - - - - - - - - - - - - -
- E - - - - E - - - - E - - - - E - - -
E E - - - E E - - - E E - - - E E - - -
- - F F - - - F F - - - F F - - - F F -
- - F - - - - F - - - - F - - - - F - -
- - - - - - - - - - - - - - - - - - -
- E - - - - E - - - - E - - - - E - - -
E E - - - E E - - - E E - - - E E - - -
- - F F - - - F F - - - F F - - - F F -
- - F - - - - F - - - - F - - - - F - -
- - - - - - - - - - - - - - - - - - -
- E - - - - E - - - - E - - - - E - - -
E E - - - E E - - - E E - - - E E - - -
- - F F - - - F F - - - F F - - - F F -
- - F - - - - F - - - - F - - - - F - -
- - - - - - - - - - - - - - - - - - -

```

c.

```

F - D D B B F - - O B B F - - O O B - F
F D D D B F F F O O B B - - O O B B - F
C D D - C F F O O E E E E E O O B B - F F
E E - C C C O O E E E E D O F F D - F C
E O O C C O O - E E - D D F F D D - F E
O O B B B - F F - B B D C C E D O B - E
O - B B - F F - B B C C C E E O B B E E
D D - C C D D E E - C C C E O C B B E E
D F - C D D - E D D - F - - C C - - E D
F F - E E O - D D - F F F F F O O - D D
F - E E O O F D - B B F F F O O B C C F
F B E E O C - E B B B - D O O B B C C F
B B E E C C E E - B B D D O O B D D - F
B O D D C - O O - - D D E E E D D - F F
F F D D O O O D F F - E E E E O O - F F
F F - O O C F F F C C F B B O O C C -
F F - O C C F - C C C B B B O C C C C -
B B - - C O E E C C D B B - C C D E E -
B B E E O O E E D D D - F F C D D E E C
- E E - O B E E D D - - F F D D O E C C

```

d.

```

F - - - - - F - - - - - F - - - - - F
F - - - - F F F - - - - - F
- - - - - F F - - E E E E - - - - F F
E E - - - - - E E E E E - - F F - - F -
E - - - - - - E E - - - F F - - - F E
- - - - - F F - - - - - E - - - - E
- - - - - F F - - - - - E E - - - E E
- F - - - - - E - - - - F - - - - E -
F F - E E - - - - - F F F F F - - - -
F - E E - - F - - - - F F F - - - - F
F - E E - - E - - - - - - - - - - F
- - E E - - E E - - - - - - - - - F
- - - - - - - - - - - - - E E E - - F F
F F - - - - - F F - - - F F - E E E E - - F F
F F - - - - F F F - - F - - - - -
F F - - - - F - - - - - - - - - -
- - - - - E E - - - - - - - - E E -
- E E - - E E - - - - F F - - - E E -
- E E - - - E E - - - - F F - - - E -

```

Figure 2:

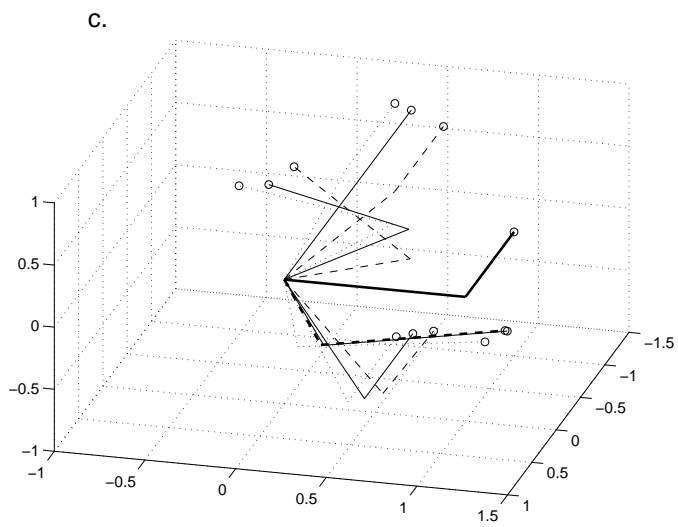
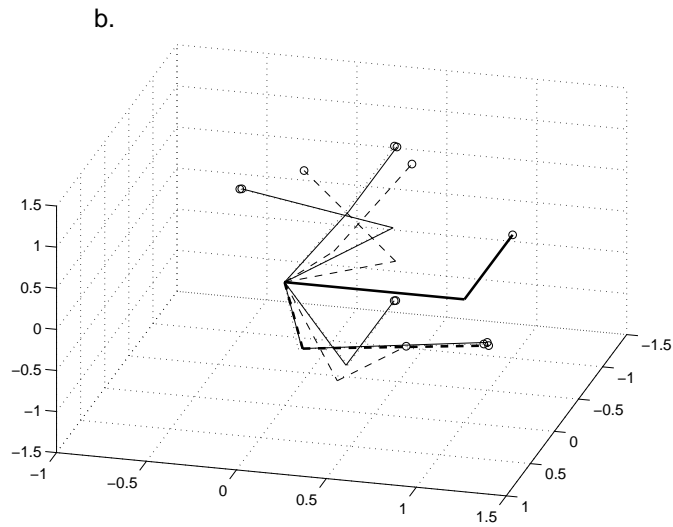
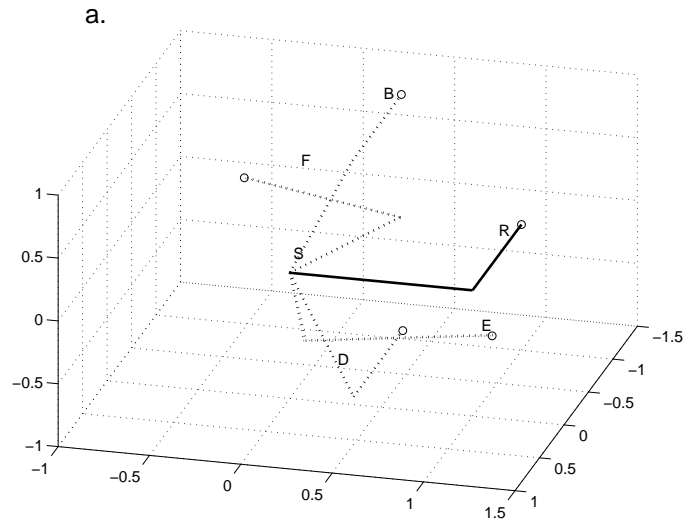


Figure 3:

a.

b.

```

D E O O D D E O O D D E O O D D E O O D      D E O O D D E O O D - - - - - O O D
E E O - D E E O - D E E O - D E E O - D      E E O - D E E - D D O O D D - E - O - D
- - F F - - - F F - - - F F - - - F F B      - - F F - - C F F O O E D F E E - F - -
C C F B B C C F B B C C F B B C C F B B      C C F B B C C F B - C C F B O D F F B -
C C - B - C C O O - D E O O - C D - - -      C C B B - E - B B - C C B O - D C B B -
D E O O D E E O - - E E - - - D E O O D      - E O O D E - - - - - - - - - E O O D
E E O - D E * * * * * - E E O - D      E E O D D - * * * * * - E E O D -
- - F F - - * * * * * - B B F F -      E - F F - - * * * * * - - - F - -
- C F B B - * * * * * - B C F B B      - - C B - - * * * * * - - F F B -
C C B B C C * * * * * - C C - B -      - C B B - - * * * * * - - C B - -
D - E O D - * * * * * - D E O O D      - E E O - - * * * * * - - E O D -
- E E D D - * * * * * - E E O - D      - E D D - - * * * * * - E E D D -
- - F F - - * * * * * - - - F F -      - - F F - - * * * * * - - - F - -
C C F B B - * * * * * B B C F B B      - C C B - - * * * * * - C C B - -
C C B B - C - - - - - B B C C - B -      - - B O - - - - - - - - - C B B O -
D E O O D D E O O D D E O O D D E O O D      - E E D D - E O O D - E - O - - E O O D
E E O F D E E O F D E E O F D E E O - D      - E - F F E E O F D E E O D D E E O D D
- - F F B B - F F - C C F F - - - F F -      - C F F B B C F F B C C F F - - - F F -
C C F - B C C F B B C - F B B C C F B B      C C - B B C C - B B C C F B - C C F B -
C C - - - C - - B - - - - B - C - - B -      C - - O - - - O O - - - B B - C C B B -

```

Figure 4:

a.

```
F - D D B B F - - O B B F - D O O B - F
F D D D B F F F O O B B - - O O B B - F
C D D - C F F O O - E E E O O B B - F F
E E - C C C O O E E E E D O F F D - F C
E O O C C O O - E E E D D F F D D F F E
O O - B B - F F B B B D C C E E O B - E
O - B B - F * * * * * E O B B E E
D D - C C D * * * * * E C B B E E
D - - C D D * * * * * C C B - E D
F F - E E O * * * * * F O O - D D
F - E E O O * * * * * O O B C C F
F B E E O F * * * * * O B B C C F
B B E E C C * * * * * O F D D - F
B O D D C E * * * * * E D D - F F
F F D D O O D D F F D E E E E O O - F F
F F - O O C F F F C C F B B O O C C -
F F - O C C F B B C C B B B O C C C C -
B B - - C O E E C C D B B - C C D E E -
B B E E O O E E D D D - F F C D D E E C
- E E - O B E E D D - - F F D D O E C C
```

b.

```
F - D - B B F - D - B B F F O O B B F
F D D - B F F - O O C - E - O O B B F F
C D D C C F F O O O E E E O O O B - F C
- - - C C - O O O E E D D - F F D D F C
E O - - E E - F F B B D C C F D D F F E
O O B E E C F F F B B C C C E E O - E E
O O B B C C * * * * * E O O B E E
- B B C C D * * * * * C C B B - D
- O O D D D * * * * * C F B B D D
- O - D D O * * * * * F F B C D -
F - E E O O * * * * * F O C C C F
F B E E O C * * * * * O O C C F F
B B E E C C * * * * * O D D - F F
B O O D B B * * * * * D D - - F -
O O D D B O D D F F E E E E E O O - - -
F F D B O O D F F F E E E E O O - C C C
F F B B C C - B B C C - - B B C C C C
F B B C C O B B C C C - B B C C D D E -
B - E E O O E E D D D B B F F D D E E -
- E E O O E E E D D - B F F F - - E B B
```

Figure 5: